# THEORETICAL MODEL OF BUOYANCY-INDUCED FLOW IN ROTATING CAVITIES

J Michael Owen and Hui Tang

Department of Mechanical Engineering

University of Bath

Bath, BA2 7AY, UK.

## ABSTRACT

The Ekman-layer equations, which have previously been solved for isothermal source-sink flow in a rotating cavity, are derived for buoyancy-induced flow. Although the flow in the inviscid core is three-dimensional and unsteady, it is assumed that the flow in the Ekman layers is axisymmetric and steady; and, as for source-sink flow, the average mass flow rate in the Ekman layers is assumed to be invariant with radius. In addition, it is assumed that the flow in the core is adiabatic, and consequently the core temperature increases with radius and with rotational speed. Approximate solutions are obtained for laminar flow, and it is shown that the Nusselt numbers for the rotating discs and the mass flow rate in the Ekman layers are proportional to $Gr_c^{1/4}$ where $Gr_c$ is a Grashof number based on the rotational Reynolds number and the temperature difference between the disc and the core. The equation for the Nusselt numbers, which includes two empirical constants, depends strongly on the radial distribution of the temperature of the discs.

**Nomenclature**

| | |
|---|---|
| $a$ | inner radius of rotor |
| $b$ | outer radius of rotor |
| $c$ | speed of sound in core |
| $Co$ | Coriolis number ($=2\frac{\lvert v_c \rvert}{\Omega r}/\beta(T_{o,b}-T_{c,b})$ |
| $C_p$ | specific heat at constant pressure |
| $C_w$ | mass flow parameter ($=\dot{m}/\mu b$) |
| $G$ | gap ratio (= s/*b*) |
| $Gr_c$ | Grashof number in model ($=Re_\phi^{\,2}\,\beta(T_{o,b}-T_{c,b})$) |

| | |
|---|---|
| $Gr_f$ | Grashof number in experiments ( $= Re_\phi^{\,2}\,\beta(T_{o,b} - T_f)$ ) |
| $h_c$ | heat transfer coefficient based on $T_c$ ( $= q_o/(T_o - T_c)$ ) |
| $h_f$ | heat transfer coefficient based on $T_f$ ( $= q_o/(T_o - T_f)$ ) |
| $I$ | integral |
| $k$ | thermal conductivity of air |
| $k_s$ | thermal conductivity of disc |
| $L$ | characteristic length |
| $\dot{m}$ | mass flow rate |
| $M$ | frictional moment on disc |
| $Ma_c$ | Mach number in core ( $\Omega_c\, b / c$ ) |
| $Nu_c$ | local Nusselt number based on $h_c$ ( $= h_c r / k$ ) |
| $Nu_f$ | local Nusselt number based on $h_f$ ( $= h_f r / k$ ) |
| $p$ | static pressure |
| $P$ | reduced pressure |
| $Pr$ | Prandtl number |
| $q_o$ | heat flux at disc surface |
| $r$ | radius |
| $R$ | gas constant |
| $Re_z$ | axial Reynolds number ( $= WL/\nu$ ) |
| $Re_\phi$ | rotational Reynolds number ( $= \rho_b \Omega b^2 / \mu$ ) |
| $Ro$ | Rossby number ( $= W / \Omega a$ ) |
| s | axial space between discs in cavity |
| $t$ | disc thickness |
| $T$ | static temperature |
| $T_c$, $T_f$, $T_o$ | temperature of core, throughflow, disc |
| $u, v, w$ | radial, tangential, axial components of velocity in rotating frame |
| $\hat{u}$ | characteristic value of $u$ in Ekman layer |
| $v_c$ | value of $v$ in core |

| | |
|---|---|
| $V_r, V_\phi, V_z$ | radial, tangential, axial components of velocity in stationary frame |
| $W$ | axial component of velocity of throughflow |
| $\chi$ | nondimensional radius ($= r/b$) |
| $x_a$ | radius ratio (= $a/b$) |
| $z$ | axial distance from disc |
| $\beta$ | volume expansion coefficient (=$1/T_{ref}$) |
| $\gamma$ | ratio of specific heats |
| $\delta$ | thickness of Ekman layer |
| $\overline{\delta}$ | nondimensional thickness of Ekman layer (=$\delta/b$) |
| $\delta T$ | temperature difference between fluid in Ekman layer and core (= $T$-$T_c$) |
| $\Delta T_{o,c}$ | temperature difference between disc and core (= $T_o$-$T_c$) |
| $\Delta T_f$ | temperature difference between disc tip and throughflow (= $T_{o,b}$-$T_f$) |
| $\eta$ | nondimensional axial distance ($= \pi z/\delta$) |
| $\theta$ | nondimensional temperature (= $(T_o - T_c)/(T_{o,b} - T_{c,b})$) |
| $\mu$ | dynamic viscosity |
| $\rho$ | density |
| $\tau_r, \tau_\phi$ | radial, tangential components of shear stress |
| $\Omega$, $\Omega_c$ | angular speed of disc, core |

*Subscripts*

| | |
|---|---|
| *a* | value at $r = a$ |
| *ad* | adiabatic |
| *b* | value at $r = b$ |
| *c* | value in core |
| *f* | value in axial throughflow |
| o | value on disc surface |
| *ref* | appropriate reference value |
| *sh* | value on shroud |

$\phi, r, z$ circumferential, radial, axial direction

## 1. INTRODUCTION

Buoyancy-induced flow in rotating cavities with an axial throughflow of air has an important effect on the clearances between the blades and casing of the high-pressure compressors in an aeroengines. Calculation of the radial growth of the corotating compressor discs involves knowledge of the flow and heat transfer inside the cavity between the discs. For buoyancy-induced flow, the inviscid flow in the core must be non-axisymmetric; for the case of hot discs and cold air, cyclonic and anti-cyclonic vortices create the necessary Coriolis forces to allow plumes (or so-called 'radial arms') of cold air to flow radially outward in the core, as shown in Fig. 1. These flows are three-dimensional, unsteady and unstable, and predictions using computational fluid dynamics (CFD) are very expensive and usually unreliable.

This paper is concerned with an approximate solution of the buoyancy-induced flow and heat transfer in rotating cavities. This involves solving the so-called linear Ekman-layer equations where, in a rotating frame of reference, the nonlinear inertial accelerations in the Navier-Stokes equations are negligible compared with the Coriolis accelerations. For the symmetrically-heated case, where the temperature in the cavity is symmetrical about its mid-axial plane, it is shown below that the average axial mass flux must be zero in the core. In this symmetrical case, the boundary layers on the discs must be nonentraining layers, referred to as Ekman layers. For the case where the buoyancy force is negligible, the equations reduce to the standard Ekman-layer equations, which have been solved for laminar and turbulent source-sink flows by Owen, Pincombe and Rogers [1].

A brief review of relevant work is given in Section 2. The Ekman-layer equations for buoyancy-induced flow are derived in Section 3, and solutions for laminar flow are given in Section 4. A summary of the main conclusions are given in Section 5.

The definitions of symbols, some of which are also defined in the text, are given in the Nomenclature. The $\phi$ coordinate is measured in the direction of rotation of the discs, $r$ is measured from the axis of rotation and $z$ from the surface of one of the discs.

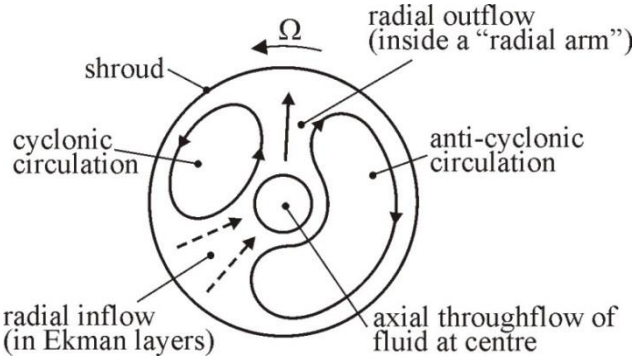


**Fig. 1 Schematic of flow structure in heated rotating cavity with axial throughflow of cooling air [ Farthing *et al.* 7]**

## 2. BRIEF REVIEW OF RELEVANT RESEARCH

A review of buoyancy-induced flow and heat transfer in open and closed rotating cavities is given by Owen and Long [2]. The work below relates only to the flow structure for the axial-throughflow case, where the Rossby number, *Ro*, has a significant effect. In addition to the papers referred to below, the books of Childs [3], Owen and Rogers [4] and Tritton [5] provide a theoretical background for a wide range of rotating flows.

The axial throughflow of air creates a toroidal vortex near the centre of the cavity, as illustrated in Fig. 2, and the radial extent of the vortex increases as the throughflow increases and as the rotational speed decreases. Owen and Pincombe [6] made flow visualization and LDA measurements under isothermal conditions, in an experimental rotating-cavity rig *without* a central shaft, with $G$ = 0.53 and $a/b$ = 0.1. Tests were conducted for $0.8 < Ro < \infty$, and it was observed that the size and strength of the toroidal vortex increased as *Ro* increased. Radially outward of the vortex, solid-body rotation occurred; inside the toroidal vortex, the recirculating flow tended to create a free-vortex, where $V_\phi / \Omega r > 1$ near the centre of the cavity; at the larger Rossby numbers, values of $V_\phi$ could be 28 times the local disc speed! The authors also observed axisymmetric and non-axisymmetric *vortex breakdown*: in the former case, the central jet expands inside the cavity; in the latter case, the jet departs from the central axis, precessing violently and creating non-axisymmetric flow inside the cavity.

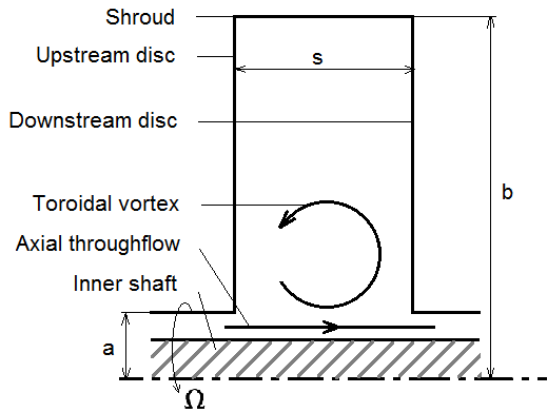


**Fig. 2 Simplified diagram of axial throughflow in an isothermal rotating cavity**

Farthing *et al.* [7, 8] carried out flow visualisation and velocity measurements in four different rotating-cavity rigs, each with $a/b \approx 0.1$. Tests were conducted over a range of gap ratios with $0.133 < G < 0.533$, and – like Owen and Pincombe – the authors observed axisymmetric and non-axisymmetric vortex breakdown. For $G \geq 0.4$, the breakdown could be dramatic, creating strong non-axisymmetric circulation with $V_\phi / \Omega r >> 1$ in the cavity. For $G \leq 0.267$, the effects of vortex breakdown were weak, and for $Ro < 20$ the fluid returned to solid-body rotation in most of the cavity.

From video recordings of the flow when one or both of the discs were heated, Farthing *et al.* [7] found that the flow in the cavity became non-axisymmetric: cyclonic and anti-cyclonic vortices were observed, as shown schematically in Fig. 1. Cold air moved radially outward in a 'radial arm', which was similar to the plume of smoke rising from a factory chimney, and flow was observed to flow radially inward in Ekman layers on the discs. The *linear equations* (see Section 3.1) were used to show that cyclonic and anti-cyclonic circulation respectively produce low and high pressure regions inside the core of rotating fluid in the cavity, and the resulting non-axisymmetric pressure provides the Coriolis forces required to produce the radial flow of air needed for the convective heat transfer. In the experiments, the rotating core of fluid precessed at a constant angular speed, $\Omega_c$, slightly less than that of the discs; the ratio of $\Omega_c/\Omega$ decreased as the temperature difference between the discs and the cooling air increased.

Owen and Powell [9] made measurements in a rig, where $a/b = 0.4$ and $G = 0.2$, and there was a central rotating shaft. The downstream disc was heated, and LDA and heat transfer measurements were made for $4 \times 10^5 < Re_\phi < 3.2 \times 10^6$ and $0.05 < Ro < 14$. Spectral analysis of the LDA measurements revealed a multi-cell structure comprising one, two or three pairs of vortices.

Long *et al.* [10, 11] tested a 70% replica of a high-pressure compressor rotor with $a/b = 0.318$, $G = 0.195$ for each cavity. As in an engine, the shrouds were heated by an external flow of hot air inside a pressurised casing, and there was an axial throughflow of cold air in the radial clearance between the cobs and a central (rotating or stationary) shaft; the radial clearance could be altered by the use of shafts of different diameter. The velocities in the cavities were measured using an LDA system, and the temperatures on the solid surfaces were measured by embedded thermocouples. Their velocity measurements, which were consistent with those made by Farthing *et al.*, showed that the Rossby number had a strong effect on the flow in the toroidal vortex at the smaller radii. Solid-body rotation (with $\Omega_c/\Omega < 1$) occurred at the larger radii, where buoyancy effects dominated.

For heated stationary cavities, there is a critical Rayleigh number (where $Ra = Pr\ Gr$) at which stably-stratified flows become unstable and buoyancy-induced flow (referred to as Rayleigh-Benard flow) occurs. For rotating cavities with an axial throughflow, although it is unclear at what conditions buoyancy-induced flow occurs, the results of Tang *et al.* [12] suggest that buoyancy effects appear to be small for $Gr < 8 \times 10^8$ . More research is needed to determine the transition to and from buoyancy-induced flow in rotating cavities.

## 3. DERIVATION OF EQUATIONS FOR BUOYANCY-INDUCED FLOW IN ROTATING CAVITIES

### 3.1 Linear equations for flow in rotating core

It is assumed here that, in contrast to the flow in the Ekman layers, the flow in the rotating core is inviscid. Although the results derived below are based on the assumption that the nonlinear inertial accelerations are negligible compared with the Coriolis accelerations, in [1] it was shown for the isothermal case that the results often apply to rotating fluids even when the inertial terms are significant.

The symbols $u, v, w$ (where $u = V_r, v = V_\phi - \Omega r,\ w = V_z$) denote the radial, tangential and axial components of velocity in a rotating frame of reference, and $p$ denotes the static pressure. The frame rotates at a constant angular speed $\Omega$ about the $z$ axis, the flow is steady and the fluid is inviscid.

In cylindrical polar coordinates for a rotating frame, the continuity equation for steady flow (or the time-average equation for unsteady flow) can be written as

$$\frac{\partial}{\partial r}(\rho u r) + \frac{\partial}{\partial \phi}(\rho v) + r\frac{\partial}{\partial z}(\rho w) = 0 \qquad (3.1)$$

If $u,v,w \ll \Omega r$, so that the nonlinear inertial terms are much smaller than the Coriolis terms, the Navier-Stokes equations reduce to

$$2\rho\Omega(v+\frac{1}{2}\Omega r)=\frac{\partial p}{\partial r} \qquad (3.2a)$$

$$2\rho\Omega u r=-\frac{\partial p}{\partial \phi} \qquad (3.2b)$$

$$\frac{\partial p}{\partial z}=0 \qquad (3.2c)$$

The Coriolis accelerations are $-2\Omega v$ and $2\Omega u$ in the radial and tangential directions respectively, and eqs (3.2 a, b & c) are referred to as the *inviscid linear equations.*

Eq (3.2b) shows that *for axisymmetric flow u = 0.* (For radial flow to occur in a rotating cavity, either it must be confined to the Ekman layers - where the Coriolis forces are produced by shear stresses – or, as discussed below, the flow must be non-axisymmetric.)

Using eq (3.2) in conjunction with eq (3.1) it follows that

$$\frac{\partial}{\partial z}[\rho\Omega(v+\frac{1}{2}\Omega r)]=0 \qquad (3.3a)$$

$$\frac{\partial}{\partial z}[\rho\Omega u r]=0 \qquad (3.3b)$$

$$\frac{\partial}{\partial z}[\rho w]=\frac{1}{2}\Omega\frac{\partial \rho}{\partial \phi} \qquad (3.3c)$$

If eq (3.3c) is circumferentially averaged, *the average axial mass flux ( $\rho w$ ) must be constant or zero*. For flows that are symmetrical about the mid-plane of the cavity (e.g. symmetrically-heated discs), it follows that the average axial mass flux must be zero. Consequently, for the symmetrical case, there can be no net entrainment into the Ekman layers on the discs, and the mass flow rate must therefore be constant.

For *incompressible flow*, eqs (3.3a,b,c) reduce to

$$\frac{\partial v}{\partial z}=0 \qquad (3.4a)$$

$$\frac{\partial u}{\partial z} = 0 \tag{3.4b}$$

$$\frac{\partial w}{\partial z} = 0 \tag{3.4c}$$

That is, the velocity is axially-stratified: there is no variation of velocity in the axial direction. This is known as the *Taylor-Proudman theorem.*

The so-called reduced pressure $P$ is defined as

$$P = p - \frac{1}{2}\rho \Omega^2 r^2 \tag{3.5}$$

and, for incompressible flow, eq (3.2a) can be expressed as

$$\frac{\partial P}{\partial r} = 2\rho \Omega v \tag{3.6}$$

So for a cyclonic vortex, where $v > 0$, $\partial P / \partial r > 0$. As in the earth's atmosphere, cyclonic circulation is therefore associated with low pressure (which increases with distance from the centre of the vortex); conversely, anti-cyclonic circulation (where $v < 0$) is associated with high pressure.

### 3.2 Ekman-layer equations for buoyancy-induced flow

This section builds on the isothermal source-sink flow equations of [1]. Only the buoyancy-induced flow in the Ekman layers radially-outward of the toroidal vortex is considered here.

In the core, which is denoted by the subscript c, pairs of cyclonic and anti-cyclonic vortices create alternating regions of low and high pressure. These generate the circumferential pressure gradient which, as shown by eq (3.2b), is required to produce a radial flow in the rotating fluid. As observed in [7] and shown in Fig. 1, it is assumed here that cold air flows radially outward from the toroidal vortex in *plumes* (or 'radial arms') in the core, and air returns radially inward inside the Ekman layers on the hot discs.

As shown in Section 3.1, if eq (3.3c) is circumferentially averaged, *the average axial mass flux ( $\rho w$ ) must be constant or zero.* Consequently, for the symmetrical case considered here – where the temperatures are the same on both discs - there can be no net entrainment into the Ekman layers on the discs. Circumferentially-

averaged velocities are used below, and the average flow rate in the Ekman layers is therefore assumed to be constant.

It follows that $\dot{m}$ , the average mass flow rate in the layer, is given by

$$\dot{m} = 2\pi r \int_0^\infty \rho u \, dz = \text{constant} \tag{3.7}$$

(The infinite upper limit of the integral is used here for consistency with the equations in Section 4.)

Eqs (3.2 a, b) apply in the core where

$$\rho_c \, \Omega^2 r(1 + 2\frac{v_c}{\Omega r}) = (\frac{\partial p}{\partial r})_c \tag{3.8a}$$

$$2\rho_c \, \Omega u_c = -\frac{1}{r}(\frac{\partial p}{\partial \phi})_c \tag{3.8b}$$

For the Ekman layer on each disc

$$\rho\Omega^2 r(1 + 2\frac{v}{\Omega r}) = \frac{\partial p}{\partial r} - \frac{\partial \tau_r}{\partial z} \tag{3.9a}$$

$$2\rho \, \Omega u = -\frac{1}{r}\frac{\partial p}{\partial \phi} + \frac{\partial \tau_\phi}{\partial z} \tag{3.9b}$$

where $\tau_r , \tau_\phi$ are the radial and tangential components of shear stress. If it is assumed that the pressure in the Ekman layer equals that in the core then it follows that the radial momentum equation becomes

$$\Omega^2 r\left[2(\frac{\rho_c v_c - \rho v}{\Omega r}) + (\rho_c - \rho)\right] = \frac{\partial \tau_r}{\partial z} \tag{3.10a}$$

and the tangential momentum equation is

$$2\,\Omega(\rho u - \rho_c u_c) = \frac{\partial \tau_\phi}{\partial z} \tag{3.10b}$$

For the isothermal case, where $\rho = \rho_c$ = constant, eqs (3.10 a, b) reduce to the equations solved in [1]. The Boussinesq approximation can be used for small temperature differences ( $\beta \delta T << 1$, where $\delta T = T - T_c$ ), so that

$$\rho = \rho_c (1 - \beta \delta T) \tag{3.11}$$

where $\beta = 1/T_{ref}$, $T_{ref}$ being an appropriate reference temperature. Eq (3.10a) can then be expressed as

$$\rho_c \Omega^2 r \left[ \beta \delta T + 2 \frac{v_c - v}{\Omega r} \right] = \frac{\partial \tau_r}{\partial z} \tag{3.12a}$$

and, as $u_c$ << u inside the layer, eq (3.10b) simplifies to

$$2 \Omega \rho_c u = \frac{\partial \tau_\phi}{\partial z} \tag{3.12b}$$

The above equations are valid for both laminar and turbulent flow in the Ekman layers, and the relevant equations for the inviscid core are discussed below.

### 3.3 Compressibility effects

Owing to the compressibility of the air in the cavity, the core temperature is assumed to increase adiabatically with radius. (This is analogous to the earth's atmosphere where, owing to gravitational acceleration, the pressure and temperature *decrease* with vertical height; the decrease in temperature is referred to as the adiabatic lapse rate [5]. However, owing to the centripetal acceleration in the rotating core, the pressure and temperature *increase* with radius.) Note: all pressures, temperatures and densities used below are circumferentially-averaged static values.

For a perfect gas

$$\frac{p_c}{\rho_c} = R T_c \tag{3.13}$$

and for adiabatic flow

$$\frac{p_c}{\rho_c^{\gamma}} = \text{constant} \tag{3.14}$$

If the angular speed of the inviscid core is $\Omega_c$ then for radial equilibrium

$$\frac{dp_c}{dr} = \rho_c \, \Omega_c^{\,2} r \tag{3.15}$$

Integration of eq (3.15) using eq (3.14) gives

$$\left(\frac{p_c}{\rho_c}\right)-\left(\frac{p_c}{\rho_c}\right)_a = \frac{\gamma-1}{2\gamma}\Omega_c{}^2 b^2 (x^2 - x_a{}^2) \tag{3.16}$$

where $x = r/b$, and $p_c = p_{c,a}$, $\rho_c = \rho_{c,a}$ at $x = x_a$. Using eq (3.13), and noting that $\gamma = C_p / C_v$ and $R = C_p - C_v$, it follows from eq (3.16) that

$$T_c - T_{c,a} = \frac{\Omega_c{}^2 b^2}{2C_p}(x^2 - x_a{}^2) \tag{3.17}$$

where $T_c = T_{c,a}$ at $x = x_a$.

Using the conventional notation of compressible flow, eq (3.17) can be expressed as

$$\frac{T_c}{T_{c,a}} = 1 + \frac{\gamma-1}{2} Ma_c{}^2 (x^2 - x_a{}^2) \tag{3.18a}$$

It can be shown that

$$\frac{p_c}{p_{c,a}} = \left[1 + \frac{\gamma-1}{2} Ma_c{}^2 (x^2 - x_a{}^2)\right]^{\gamma/(\gamma-1)} \tag{3.18b}$$

and

$$\frac{\rho_c}{\rho_{c,a}} = \left[1 + \frac{\gamma-1}{2} Ma_c{}^2 (x^2 - x_a{}^2)\right]^{1/(\gamma-1)} \tag{3.18c}$$

The Mach number in the core, $Ma_c$, is defined as

$$Ma_c = \frac{\Omega_c b}{c} \tag{3.19}$$

and the speed of sound, $c$,

$$c = \sqrt{\gamma R T_{c,a}} \tag{3.20}$$

Despite the fact that eqs (3.18a,b&c) have a similar form to the ratio of total to static values associated with nonrotating compressible flow, the pressures, temperatures and densities in these equations are static values. For air, it is usually assumed that $\gamma$ = 1.4, which is the ratio of the specific heats. Strictly, this is valid only for

isentropic (reversible and adiabatic) flow, whereas in practice the flow will be nonisentropic. Consequently, it may be appropriate to use a value less than 1.4 for $\gamma$ when applying the above equations to experimental data. This is discussed further in Section 4.1.

## 4. SOLUTION OF EKMAN-LAYER EQUATIONS FOR LAMINAR FLOW

### 4.1 Assumed distribution of velocity and temperature

Fig. 3 shows the assumed flow structure for the model. As the flow is radially inward in the Ekman layer on a heated rotating disc, u will be taken as positive in the negative radial direction. It is assumed that, as used in[1] for isothermal laminar Ekman-layer flow,

$$u = \hat{u}\, e^{-\eta} \sin\eta \tag{4.1a}$$

and

$$v_c - v = v_c e^{-\eta} \cos\eta \tag{4.1b}$$

where

$$\eta = \pi z / \delta \tag{4.1c}$$

so that $\eta = \pi$ when $z = \delta$, $\delta$ being a convenient thickness of the Ekman layer. When $\eta \to \infty, u = 0, v = v_c$. Note that $\hat{u} = \hat{u}(x), v_c = v_c(x)$, where $x = r / b$, and the shapes of the velocity profiles are shown in Fig. 4.

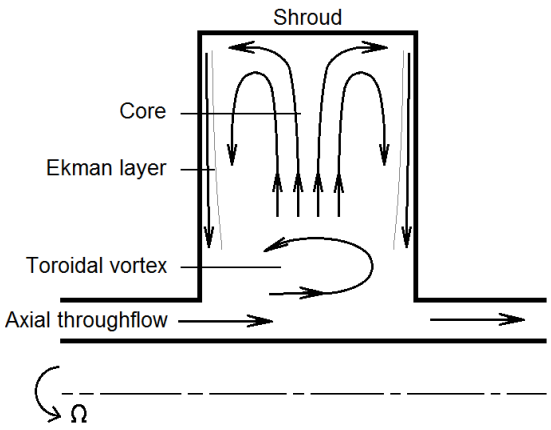


**Fig. 3 Assumed flow structure**

It is also assumed that $\delta T$ has the same form as the tangential velocity distribution in the Ekman layer, so that

$$\delta T = \Delta T_{o,c}\, e^{-\eta} \cos\eta \qquad (4.2)$$

where $\delta T = T - T_c$ and $\Delta T_{o,c} = T_o - T_c$, $T_c$ and $T_o$ and being the temperatures of the core and the surface of the rotating disc respectively. When $\eta \to \infty, T = T_c, \partial T / \partial \eta = 0$, and the radial variation of $T_c$ is given by eq (3.17).

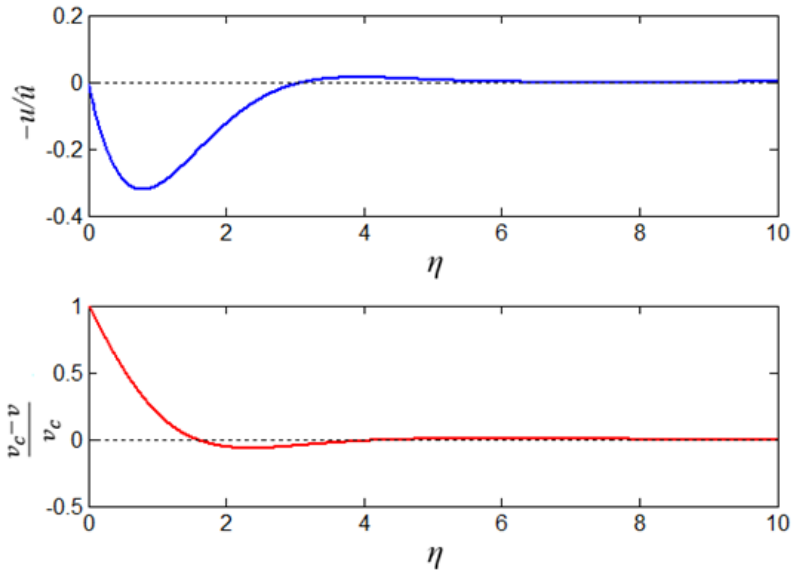


**Fig. 4 Assumed shape of velocity distributions in Ekman layer**

Some comments about the choice of profiles is needed here. It may seem strange to assume that the flow in the Ekman layers could be laminar at engine-operating conditions, where Grashof numbers of O($10^{12}$) are common. However, Coriolis forces can delay the onset of transition from laminar to turbulent flow in rotating cavities. For example, Bohn *et al.* [13] correlated their measured Nusselt numbers for the shroud for buoyancy-induced flow in a closed rotating cavity, for Grashof numbers up to $10^{12}$, with $Gr^{0.22}$, which is closer to the laminar exponent of 1/4 than to the turbulent one of 1/3. Farthing *et al.* [8] correlated their measured Nusselt numbers for the disc for buoyancy-induced flow in a rotating cavity with axial throughflow, for Grashof numbers up to $10^{11}$, with $Gr^{0.25}$. It is unclear when transition occurs for buoyancy-induced flow in rotating cavities.

The oscillatory nature of the velocity distributions, created by the exponentially-decaying sine and cosine functions shown in Fig. 4, may also seem strange to some readers but it has been observed to occur in laminar source-sink flow in rotating cavities [14]. As shown in [4], there is a strong analogy between the transfer of heat

and angular momentum in rotating cavities, and consequently the axial distributions of temperature and tangential velocity tend to be similar.

To apply the model, it is necessary to decide whether or not heat is transferred from the Ekman layer to the core. *If heat is not transferred to the core*, the enthalpy of the fluid in the Ekman layer must increase as it flows radially inward. This implies that $\Delta T$ must increase as *x* decreases: experiments, in which $T_o$ decreases as *x* decreases, suggest the contrary. *If heat is transferred to the core*, this beg the question: As the axial gradient of temperature tends to zero at the edge of the Ekman layer, how could this heat transfer occur? A possible answer is that, although the *average* axial mass flux is zero, eq (3.3c) shows that the *local* flux varies circumferentially: this would allow convection of enthalpy into the core.

In the solutions presented below, it is implicitly assumed that heat *is* transferred to the core. This will increase the enthalpy of the axial throughflow, which will put a constraint on the application of the solutions to a real problem: there must be a limit to the temperature rise of the throughflow beyond which buoyancy-induced flow cannot occur in the cavity. (Although heat transfer occurs from the disc to the air in the core, it is assumed that there is no significant heat transfer between the radial plumes of air and the cyclonic and anti-cyclonic vortices in the core. As assumed in Section 3.3, the circumferential-average temperature of the core can be considered to increase adiabatically with radius.)

### 4.2 Calculation of thickness of Ekman layer

For laminar flow, the radial momentum equation eq (3.12a) becomes

$$\rho_c \Omega^2 r \left[ \beta \delta T + 2 \frac{v_c - v}{\Omega r} \right] = \mu \frac{\partial^2 u}{\partial z^2} \tag{4.3}$$

Using the Boussinesq approximation (when $\beta \delta T << 1$), the density can be approximated by

$$\rho = \rho_c (1 - \beta \delta T) \tag{4.4}$$

Using this approximation, and neglecting second-order density variations, eq (4.3) can be integrated across the layer to give

$$\rho_c \Omega^2 r \int_0^\infty \left[ (\beta \Delta T_{o,c} + 2 \frac{v_c}{\Omega r}) e^{-\eta} \cos \eta \right] d\eta = \frac{\pi^2 \mu}{\delta^2} \left( \frac{\partial u}{\partial \eta} \right)_o \tag{4.5}$$

where $\eta = \pi z / \delta$ and the subscript o denotes the disc surface at $\eta = 0$. It follows that

$$\frac{1}{2}\rho_c \Omega^2 r\,[\beta \Delta T_{o,c} + 2\frac{v_c}{\Omega r}] = \frac{\pi^2 \mu}{\delta^2}\hat{u} \tag{4.6}$$

Using eq (3.7), the mass flow rate is given by

$$\dot{m} = 2r\delta \int_0^\infty \rho u \, d\eta \tag{4.7}$$

From eqs (4.1a) and (4.4), eq (4.7) becomes

$$\dot{m} = r\,\rho_c \delta \hat{u}(1 - \frac{1}{4}\beta \Delta T_{o,c}) \approx r\,\rho_c \delta \hat{u} \tag{4.8}$$

and the variation of $\rho_c$ with radius is given by eq (3.18c).

Eliminating $\hat{u}$ from eqs (4.6) and (4.8), it follows that

$$\beta \Delta T_{o,c}\left(1 + 2\frac{v_c}{\Omega r}\frac{1}{\beta \Delta T_{o,c}}\right) = 2\frac{\pi^2 \dot{m}\mu}{\Omega^2 r^2 \rho_c{}^2 \delta^3} \tag{4.9}$$

In practice $v_c < 0$, so that the Coriolis force opposes the buoyancy force and reduces the mass flow rate in the Ekman layer. Also, in practice $|v_c| / \Omega r$ is invariant with radius for buoyancy-induced flow, and it is assumed that $2|v_c| / \Omega r < \beta \Delta T_{o,c} << 1$.

Eq (4.9) can be rearranged to give

$$\bar{\delta} = \left[2\pi^2 \frac{C_w}{Gr_c(\theta - Co)}\left(\frac{\rho_{c,b}}{\rho_c}\right)^2 \frac{1}{x^2}\right]^{1/3} \tag{4.10}$$

where

$$\bar{\delta} = \frac{\delta}{b} \tag{4.11a}$$

$$C_w = \frac{\dot{m}}{\mu b} \tag{4.11b}$$

$$Gr_c = Re_\phi{}^2 \beta (T_{o,b} - T_{c,b}) \tag{4.11c}$$

$$\mathrm{Re}_\phi = \frac{\rho_b \Omega b^2}{\mu} \tag{4.11d}$$

$$Co = 2\frac{|v_c|}{\Omega r}\frac{1}{\beta(T_{o,b} - T_{c,b})} \tag{4.11e}$$

$$\theta = \frac{T_o - T_c}{T_{o,b} - T_{c,b}} \tag{4.11f}$$

For simplicity, $\mu$ and $\beta$ are assumed to be constant, and the density ratio in eq (4.10) can be calculated using eq *(3.18c). Note that Co, the Coriolis number, is an empirical constant that must be less than unity.*

### 4.3 Calculation of flow rate in Ekman layer

The fluid enters the core in radial plumes and leaves via the Ekman layer. It is assumed that the frictional moment, *M*, on the rotating disc, between *r = a* and *r = b*, provides the increase in angular momentum between the fluid in the plumes entering the core and the fluid in the Ekman layer leaving the cavity. Treating the plumes and the Ekman layer as a continuous stream tube, the angular momentum equation can be expressed as

$$M = \dot{m}\, a\,(V_{\phi,out} - V_{\phi,in}) \tag{4.12}$$

where $V_{\phi,in}$ and $V_{\phi,out}$ are the bulk-average tangential components of velocity, in a stationary frame of reference, of the fluid in the plumes and the Ekman layer respectively. At inlet to the plumes

$$V_{\phi,in} = v_c + \Omega a = \Omega a\,(1 - \frac{|v_c|}{\Omega a}) \tag{4.13}$$

At outlet from the Ekman layer,

$$V_{\phi,out} = v_{out} + \Omega a \tag{4.14a}$$

where

$$v_{out} = \frac{2\pi a}{\dot{m}}\int_0^\infty \rho u v\, dz \tag{4.14b}$$

and

$$\int_0^\infty \rho u v dz \approx \frac{\rho_c \delta \hat{u} v_c}{\pi} \int_0^\infty e^{-\eta} \sin\eta (1 - e^{-\eta} \cos\eta) d\eta = \frac{3}{8\pi} \rho_c \delta \hat{u} v_c \tag{4.15}$$

Hence, using eq (4.8),

$$v_{out} = \frac{3}{4} v_c \tag{4.16}$$

Consequently,

$$V_{\phi,out} - V_{\phi,in} = \frac{1}{4} |v_c| \tag{4.17}$$

and using

$$\frac{|v_c|}{\Omega r} = \frac{\Omega - \Omega_c}{\Omega} \tag{4.18}$$

it follows that

$$M = \dot{m} a (V_{\phi,out} - V_{\phi,in}) = \frac{1}{4} \dot{m} a^2 (\Omega - \Omega_c) \tag{4.19}$$

The frictional moment on the disc is given by

$$M = 2\pi \int_a^b r^2 \tau_\phi dr \tag{4.20}$$

where, using eqs (4.1b) and (4.1c),

$$\tau_\phi = \mu \left( \frac{\partial V_\phi}{\partial z} \right)_o = -\pi \frac{\mu}{\delta} \left( \frac{\partial v}{\partial \eta} \right)_o = \pi \frac{\mu |v_c|}{\delta} \tag{4.21}$$

Hence

$$M = 2\pi^2 \mu (\Omega - \Omega_c) b^3 \int_{x_a}^1 x^3 \bar{\delta}^{-1} d x \tag{4.22}$$

Equating eqs (4.19) and (4.22), it follows that

$$C_w = 8\pi^2 x_a^{-2} \int_{x_a}^1 x^3 \bar{\delta}^{-1} d x \tag{4.23}$$

Using eq (4.10) for $\bar{\delta}$ , eq (4.23) becomes

$$C_w = 8\pi^2 x_a^{-2} \int_{x_a}^{1} x^{11/3} \left[ \frac{1}{2\pi^2} \frac{Gr_c(\theta - Co)}{C_w} \left( \frac{\rho_c}{\rho_{c,b}} \right)^2 \right]^{1/3} dx \qquad (4.24)$$

Rearranging eq (4.24)

$$C_w = 4\pi x_a^{-3/2} I^{3/4} Gr_c^{1/4} \qquad (4.25)$$

where

$$I = \int_{x_a}^{1} x^{11/3} \left[ (\theta - Co) \left( \frac{\rho_c}{\rho_{c,b}} \right)^2 \right]^{1/3} d\,x \qquad (4.26)$$

It follows from eq (4.10) that

$$\bar{\delta} = 2\pi \frac{I^{1/4}}{x_a^{1/2} Gr_c^{1/4}} \left[ \frac{1}{(\theta - Co)} \left( \frac{\rho_{c,b}}{\rho_c} \right)^2 \frac{1}{x^2} \right]^{1/3} \qquad (4.27)$$

**4.4 Calculation of Nusselt numbers**

In the theoretical model, the local heat transfer coefficient $h_c$ , using $T_c$ as the reference temperature, is defined as

$$h_c = \frac{q_o}{\Delta T_{o,c}} = \frac{q_o}{T_o - T_c} \qquad (4.28a)$$

where $q_o$ is the heat flux at the disc surface. In most experiments, where $T_c$ is unknown, the heat transfer coefficient $h_f$ is defined as

$$h_f = \frac{q_o}{T_o - T_f} \qquad (4.28b)$$

where $T_f$ is the temperature of the axial thoughflow. It follows that if the heat fluxes are equal in these definitions then

$$\frac{h_f}{h_c} = \frac{T_o - T_c}{T_o - T_f} \qquad (4.29)$$

The heat flux is given by

$$q_o = -k\left(\frac{\partial T}{\partial z}\right)_o = -\pi\frac{k}{\delta}\left(\frac{\partial T}{\partial \eta}\right)_o \tag{4.30}$$

Using eq (4.2), eq (4.28a) becomes

$$h_c = \pi\frac{k}{\delta} = \pi\frac{k}{b\bar{\delta}} \tag{4.31}$$

It follows from eq (4.27) that $Nu_c$, the local Nusselt number based on $h_c$, is

$$Nu_c = \frac{h_c r}{k} = \frac{1}{2}\frac{x_a^{1/2}}{I^{1/4}}Gr_c^{1/4}\left[(\theta - Co)\left(\frac{\rho_c}{\rho_{c,b}}\right)^2 x^5\right]^{1/3} \tag{4.32}$$

where the integral $I$ is given by eq (4.26).

In most experiments, the local Nusselt number, $Nu_f$, is based on $h_f$, and it follows from eq (4.29) that

$$Nu_f = \frac{h_f r}{k} = \frac{T_o - T_c}{T_o - T_f}Nu_c \tag{4.33}$$

and the experimental Grashof number, $Gr_f$, is usually defined as

$$Gr_f = Re_\phi^{\,2}\,\beta\,\Delta T_f \tag{4.34}$$

where $\Delta T_f = T_{o,b} - T_f$. $Gr_f$ can be increased by increasing either $Re_\phi$ or $\Delta T_f$. However, it can be shown from eqs (3.17) and (4.33) that, owing to the adiabatic temperature rise in the core, $T_c$ increases and $Nu_f$ consequently decreases as $Re_\phi$ increases. *This means that the same value of $Gr_f$ can result in different values of $Nu_f$, and it is possible for an increase in $Gr_f$ to result in a decrease in $Nu_f$*. This paradoxical behaviour has been observed by Tang *et al.* [12].

## 5. CONCLUSIONS

The Ekman-layer equations, which have previously been solved for isothermal source-sink flow in a rotating cavity, have been extended to buoyancy-induced flow. The principal assumption is that, although the flow in the inviscid core is three-dimensional and unsteady, the average flow in the Ekman layers is axisymmetric and

steady. As for source-sink flow, the average mass flow rate in the Ekman layers is assumed to be invariant with radius. In addition, it is assumed that the flow in the core is adiabatic, and consequently the core temperature is proportional to $\Omega_c^2 r^2$.

The solutions for laminar flow show that the mass flow rate in the Ekman layer is proportional to $Gr_c^{1/4}$ (where $Gr_c = \mathrm{Re}_\phi^2 \beta(T_{o,b} - T_{c,b})$ and $Re_\phi$ is the rotational Reynolds number); the thickness of the Ekman layer is proportional to $Gr_c^{-1/4}$. The solutions also show that $Nu_c$, the local Nusselt number based on the core temperature, is proportional to $Gr_c^{1/4}$.

As the core temperature increases as $Re_\phi$ increases, it is possible for an increase in $Gr_f$, the experimental Grashof number, to result in a *decrease* in $Nu_f$, the measured Nusselt number.

**REFERENCES**


1. Owen, J.M., Pincombe, J.R. and Rogers, R.H. 1985. Source-sink flow inside a rotating cylindrical cavity. J. Fluid Mech. 155, pp 233-265.
2. Owen, J.M. and Long, C.A. 2015 Review of buoyancy-induced flow in rotating cavities. ASME J. Turbomach. Accepted for publication.
3. Childs, P.R.N. 2011. Rotating Flow, Elsevier, Oxford.
4. Owen, J. M. and Rogers, R. H. 1995, Flow and Heat Transfer in Rotating Disc Systems, Volume 2 – Rotating Cavities. Research Studies Press, UK; John Wiley, N.Y.
5. Tritton, D.J. 1988. Physical fluid dynamics. OUP, New York.
6. Owen, J.M. and Pincombe, J.R. 1979. Vortex breakdown in a rotating cylindrical cavity. J. Fluid Mech., 90, pp. 109-127.
7. Farthing, P.R., Long, C.A., Owen, J.M. and Pincombe, J.R. 1992. Rotating cavity with axial throughflow of cooling air: flow structure. ASME J. Turbomach, 114, pp. 237-246.
8. Farthing, P.R., Long, C.A., Owen, J.M. and Pincombe, J.R. 1992. Rotating cavity with axial throughflow of cooling air: heat transfer. ASME J. Turbomach, 114, pp. 229-236.
9. Owen, J.M. and Powell, J., 2006. Buoyancy-induced flow in a heated rotating cavity. ASME J. Eng. Gas Turbines & Power, 128, pp 128-134.

**10.** Long, C.A., Miche, N.D.D. and Childs, P.R.N., 2007. Flow measurements inside a heated multiple rotating cavity with axial throughflow. Int.J.Heat Fluid Flow,28, pp 1391-1404.

**11.** Long, C.A. and Childs, P.R.N., 2007. Shroud heat transfer measurements inside a heated multiple rotating cavity with axial throughflow. Int.J.Heat Fluid Flow, 28, pp 1405-1417.

**12.** Tang, H., Shardlow, T., and Owen, J.M., 2015. Use of fin equation to calculate Nusselt numbers for rotating discs. ASME Paper GT2015-42029. Accepted for publication in ASME J. Turbomach.

**13.** Bohn, D., Deuker, E., Emunds, R. and Gorzelitz, V. 1995. Experimental and theoretical investigations of heat transfer in closed gas filled rotating annuli. ASME J. Turbomach, 117, pp. 175-183.

**14.** Owen, J.M. and Pincombe, J.R. 1980. Velocity measurements inside a rotating cylindrical cavity with a radial outflow of fluid. J.Fluid Mech. 99, 111-127.